White Rose Research Online

eprints@whiterose.ac.uk
https://eprints.whiterose.ac.uk
Universities of Leeds, Sheffield and York

Deposited via The University of Leeds.

White Rose Research Online URL for this paper:
https://eprints.whiterose.ac.uk/id/eprint/80291/

Version: Accepted Version

Article:
Henkelis, JJ, Ronson, TK and Hardie, MJ (2014) Lanthanide coordination polymers with pyridyl-N-oxide or carboxylate functionalised host ligands. CrystEngComm, 16 (18). 3688 - 3693. ISSN: 1466-8033

https://doi.org/10.1039/c3ce40776d

Reuse
Items deposited in White Rose Research Online are protected by copyright, with all rights reserved unless indicated otherwise. They may be downloaded and/or printed for private study, or other acts as permitted by national copyright laws. The publisher or other rights holders may allow further reproduction and re-use of the full text version. This is indicated by the licence information on the White Rose Research Online record for the item.

Takedown
If you consider content in White Rose Research Online to be in breach of UK law, please notify us by emailing eprints@whiterose.ac.uk including the URL of the record and the reason for the withdrawal request.

UNIVERSITY OF LEEDS
University of Sheffield
UNIVERSITY of York

CrystEngComm

RSCPublishing

ARTICLE

Tuning the coordination chemistry of cyclotriveratrylene ligand pairs through alkyl chain aggregation†

Cite this: DOI: 10.1039/x0xx00000x

James J. Henkelis and Michaele J. Hardie*

Received 00th January 2012,
Accepted 00th January 2012

DOI: 10.1039/x0xx00000x

www.rsc.org/crystengcomm

Propylated cyclotriveratrylene (CTV) ligands display different coordination chemistry over their methylated congeners as a result of increased solubility, an affinity for alkyl chain aggregation and steric factors. The propylated ligand *tris*(isonicotinoyl)-*tris*(propoxy)-cyclotricatechylene (**L1p**) forms a 1D coordination polymer within complex $\{[Ag(\mathbf{L1p})[Co(C_2B_9H_{11})_2]](DMF)\}_\infty$ (complex **1p**), and a 2D sheet of $4{\cdot}8^2$ topology in $\{[Cd(\mathbf{L1p})(ONO_2)_2(H_2O)]\cdot(DMF)\cdot 0.5(Et_2O)\}_\infty$ (complex **2p**), neither of which are formed with the analogous methylated ligand *tris*(isonicotinoyl)-cyclotriguaiacylene (**L1m**). Both complexes **1p** and **2p** display multiple sites of aggregation of hydrophobic groups. The new propylated ligand *tris*(2-quinolylmethyl)-*tris*(propoxy)-cyclotricatechylene (**L2p**) forms a 1D coordination polymer with Ag(I) in complex$\{[Ag_2(\mathbf{L2p})_2][Co(C_2B_9H_{11})_2]_2\cdot 1.5(MeNO_2)\}_\infty$ (complex **3p**) and a novel, compressed octahedral structure with palladium(II) cations, $[Pd_6(\mathbf{L2p})_4(CF_3CO_2)_{12}]$ (complex **4p**). Neither complex was accessible with the methylated congener *tris*(2-quinolylmethyl)-cyclotriguaiacylene (**L2m**).

1. Introduction

The ability of suitably pre-functionalised building blocks to recognise each other in solution and spontaneously self-assemble to form a complex is well understood.[1,2] Discrete coordination cages and infinite coordination networks of increasing complexity have been prepared utilising the self-assembly of multifunctional ligands and metal cations,[3-5] and their applications range from catalysis [6-10] to sophisticated guest incarceration.[11-13]

The study of sterically and interactionally similar ligand sets has garnered much interest due to their ability to selectively form homo- and heteroleptic complexes, allowing the formation of structures ordinarily inaccessible with a single ligand system.[14-16] This phenomenon relies on a sliding scale of kinetic stability, whereby the dynamic nature of the coordination bond can be either exploited to enable ligand exchange, or relied upon for kinetic stability.[17] The tailoring of organic ligands and assembly conditions allows the chemist to exercise a degree of control over their self-assembly.[18-19] Fujita and co-workers, for example, have demonstrated an intricate system where small alterations to bridging ligand bite angle are enough to effect a large structural change between $M_{12}L_{24}$ and $M_{24}L_{48}$ polyhedra.[20] Likewise, the groups of Stang and Yamaguchi have shown how multi-ligand systems can undergo reversible exchange at room temperature to afford a variety of products.[21-23] Alternatively, Ward and co-workers have shown how a sterically and interactionally similar ligand pair of multidentate pyridine-pyrazole ligands can each self-assemble into a tetrahedral complex when a templating tetrahedral anion is used;[24] yet heteroleptic complexes are formed when largely different ligand systems are employed in direct competition.

London dispersion forces represent the weakest van der Waals interactions between molecules [25,26] and, whilst they are ubiquitous in nature, they are generally overlooked with respect to metallo-supramolecular chemistry due to the higher comparative strength of ion-ion and ion-dipole interactions.[27-29] Such dispersive interactions are usually exhibited as part of the hydrophobic effect,[30-31] which helps describe how and why proteins fold, alongside the mechanics of membranes.[32,33] Their contribution to self-assembly can be significant, however, and Cockroft and co-workers have presented experimental measurements describing how cohesive solvent interactions, otherwise known as solvophobic effects, play a strong and dominant role in driving the reorganisation and aggregation of apolar surfaces in solution.[34]

Our research concerns derivatives of the relatively rigid and macrocyclic cavitand, cyclotriveratrylene (CTV). Its open upper rim allows for facile functionalisation, whereby donor moieties may be appended to afford ligands. Tripodal derivatives such as those shown in Scheme 1 are chiral.

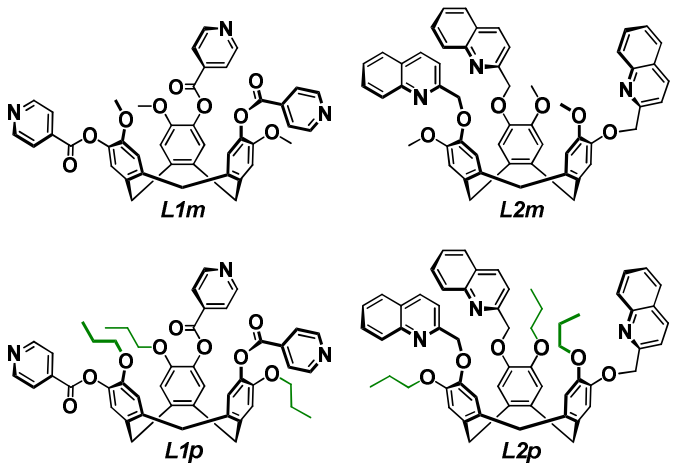

Scheme 1 Molecular structures of 4-pyridyl (**L1m**, **L1p**) and 2-quinolyl (**L2m**, **L2p**) ligand pairs utilised in the study.

The self-assembly of derivatised CTVs with metal cations is well established, and coordination polymers,[35-37] discrete metallo-cages,[38-42] and mechanically interlocked architectures [43-45] are known. However, the chemistry of mixed ligand systems is generally limited to the solution-phase, and we have recently demonstrated how the formation and manipulation of homo- and heteroleptic $[Pd_6L_8]^{12+}$ octahedral cages can be controlled with high fidelity.[46] These represent examples in which both ligands are suitably pre-designed to undergo metal-mediated self-assembly to afford structurally analogous complexes.

Herein we report a study of two interactionally and sterically similar ligand pairs which do not self-assemble to form identical complexes, and instead show dissimilar coordination chemistry which is driven, in part, by aggregation effects.

2 Results and discussion

Ligands (±)-*tris*(isonicotinoyl)-cyclotriguaiacylene (**L1m**), (±)-*tris*(isonicotinoyl)-*tris*(propoxy)-cyclotricatechylene (**L1p**) and (±)-*tris*(2-quinolylmethyl)-cyclotriguaiacylene (**L2m**) were prepared according to literature procedures.[47-50] The previously unreported ligand (±)-*tris*(2-quinolylmethyl)-*tris*(propoxy)-cyclotricatechylene (**L2p**) was prepared through reaction of propylated-cyclotriguaiacylene (*p*-CTG)[46] with 2-chloromethylquinoline in basic acetonitrile (MeCN), using an adapted version of a previously reported procedure, and isolated as a racemic mixture in high yields.[47] Ligands **L1m**, **L1p**, **L2m** and **L2p** were employed as racemic mixtures for all coordination studies and their molecular structures can be seen in Scheme 1. Whilst individual ligand pairs are essentially isostructural and differ only by the length of *ortho*-alkoxy substituents, we postulate that their dissimilar coordination chemistry may be attributable, in part, to aggregation effects present in the complexes of the longer-chained ligands.

2.1 Aggregation as a directing interaction

In our hands ligands crystalline complexes of **L1m** or **L1p** and silver(I) cations were only isolated with the bulky cobalt(III) *bis*(dicarbollide) counter-anion, $[Co(C_2B_9H_{11})_2]^-$. This bulky and weakly coordinating anion may have a structure-directing effect on coordination polymer formation,[51,52] and we have previously reported that methylated ligand **L1m** forms an intertwined 1D polymeric structure when crystallized with $Ag[Co(C_2B_9H_{11})_2]$ from an acetonitrile (MeCN) solution, $\{[Ag(\mathbf{L1m})_2][Co(C_2B_9H_{11})_2]\cdot 6(MeCN)\}_\infty$, complex **1m**, Figure 1b.[48] Propylated ligand **L1p**, under similar conditions, affords a different 1D polymer whose formation may be facilitated by aggregation of propyl moieties. Such aggregation was also evident in the previously reported crystal structure of ligand **L1p**, whereby six individual ligands were observed to pack to create a highly hydrophobic pocket that is filled with six, inwardly-orientated propyl chains, Figure 1a.[46]

The stoichiometric reaction of propylated ligand **L1p** and $Ag[Co(C_2B_9H_{11})_2]$ in *N,N'*-dimethylformamide (DMF) afforded complex $\{[Ag(\mathbf{L1p})[Co(C_2B_9H_{11})_2]]\cdot 2.5(DMF)\cdot(H_2O)\}_\infty$ **1p**, which features a 1-D coordination polymer. Single crystals were grown by diffusing diethyl-ether vapours into the DMF solution and the structure was elucidated using synchrotron radiation. The structure was solved in the triclinic space group *P*-1 to display the asymmetric unit contents as a molecule of both ligand **L1p** and $[Co(C_2B_9H_{11})_2]^-$, each coordinated to a silver(I) centre, alongside solvent molecules. Host-guest interactions are present between a DMF molecule and ligand **L1p**, where the solvent molecule is non-covalently bound by the hydrophobic cavity of the host ligand. Analogous host-guest behaviour was reported for complex **1m** with acetonitrile solvent.[48]

In complex **1p**, individual **L1p** ligands coordinate to three symmetry-equivalent silver(I) centres, all of which are of distorted tetrahedral geometry, and the $[Co(C_2B_9H_{11})_2]^-$ anion coordinates to the metal centre through a hydridic interaction. Pyridyl N-Ag and (B)H-Ag bond lengths were measured at 2.264(4), 2.280(4) and 2.176 Å, respectively, alongside N-Ag-N bond angles of 127.48(14), 101.76(14) and 97.97(13) °. This is contrasting behaviour to that observed for complex **1m**, where silver(I) centres were coordinated by four pyridyl donors and the $[Co(C_2B_9H_{11})_2]^-$ anion remained uncoordinated, Figure 1b.[48] Symmetry expansion of complex **1p** gives rise to a 1D ladder-type motif, whereby **L1p** ligands are all inwardly orientated to afford a quasi-cylindrical arrangement of head-to-head ligands. Individual ligands are of the same enantiomer, rendering each 1D polymer homochiral. The inwardly orientated ligand arrangement gives rise to small pockets of space which are filled with solvent of crystallization. In comparison to individual coordination polymers of complex **1m**, individual **L1m** ligands are only 2-coordinate and the third ligand arm acts to interdigitate neighbouring 1D chains to afford the extended, intertwined structure, Figure 1b.[48]

The individual 1D 'cylinders' of complex **1p** again exhibit aggregation of propyl chains, where the inwardly orientated propyl moieties aggregate across the polymer akin to the rungs of a ladder. Such interactions act to sculpt the shape of individual 1D polymers and, alongside the coordinating $[Co(C_2B_9H_{11})_2]^-$ anion, drive the expansion of the 1D polymer from 2-connected, as seen for complex **1m**, to 3-connected, Figure 1c.[48] There is no evidence for further

 This journal is © The Royal Society of Chemistry 2012

intermolecular interactions between individual 1D polymers. In a similar manner to complex **1m**, the extended structure of complex **1p** features back-to-back π-stacking of **L1p** ligands, of a neighbouring 1D chains, and displays aromatic centroid separations of 3.856 Å. The result is a densely packed extended lattice with solvent DMF in the interstitial sites. The composition of complex **1p** was confirmed with IR spectroscopy and combustion analysis.

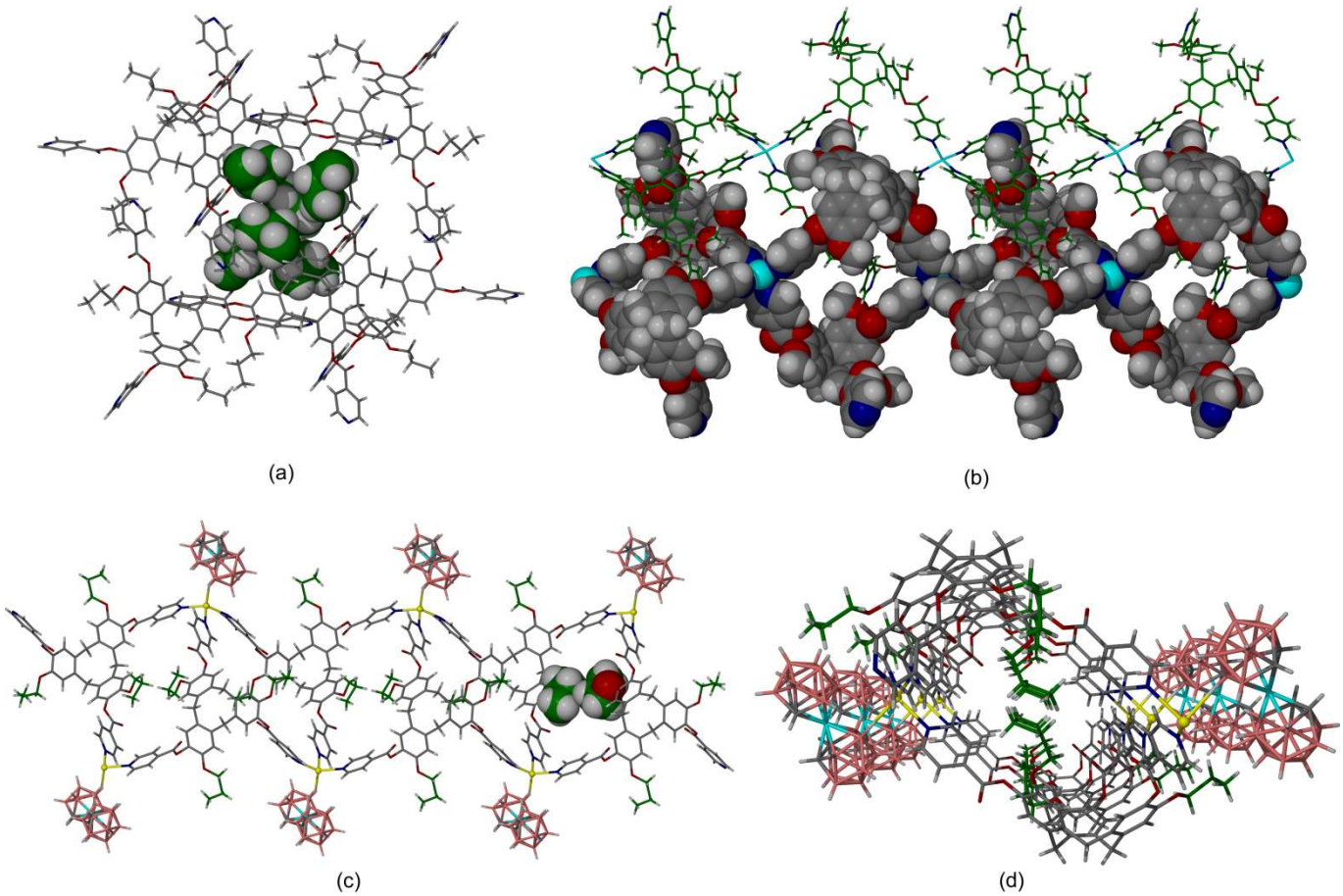

Fig. 1 (a) Taken from the crystal structure of ligand **L1p**, displaying the aggregation of six ligands based on interactions between hydrophobic propyl moieties. Propyl chains are coloured green and displayed in space-filling mode for clarity;[46] (b) our previously reported intertwining 1D network, $\{[Ag(\mathbf{L1m})_2][Co(C_2B_9H_{11})_2]\cdot 6(MeCN)\}_\infty$, complex **1m**, as viewed down the crystallographic *c* axis. Individual 1D chains are colour coded for clarity. Solvent acetonitrile and $[Co(C_2B_9H_{11})_2]^-$ anions are omitted;[48] (c) from the crystal structure of complex **1p** (this study), displaying aggregation of the hydrophobic propyl moieties across the 1D ladder; (d) complex **1p**, as viewed down the crystallographic *b* axis, highlighting the inwardly orientated arrangement of ligands and aggregation of propyl chains. Propyl chains are coloured green for clarity.

The stoichiometric reaction of **L1p** and $Cd(NO_3)_2$ in DMF, and subsequent diffusion of diethyl-ether vapours into the reaction mixture, resulted in the formation of complex $\{[Cd(\mathbf{L1p})(ONO_2)_2(H_2O)]\cdot(DMF)\cdot 0.5(Et_2O)\}_\infty$ **2p**. Complex **2p** features a 2D network, and aggregation of the hydrophobic groups is again apparent in the structure. The crystal structure was solved in the monoclinic space group *C*2/*c*, and the asymmetric unit was a molecule of **L1p**, coordinating a cadmium(II) centre with two chelating nitrates and one molecule of coordinated water, alongside a molecule of solvent DMF and half a molecule of diethyl-ether. The structure showed considerable disorder which is described in Supplementary Information, and only one of the disordered positions is depicted in Figure 2 for the sake of clarity. Each **L1p** ligand coordinates the Cd(II) centre with N-Cd bond lengths between 2.335(8) and 2.456(12) Å. The Cd(II) centre has octahedral geometry and is *facially* coordinated by **L1p** ligands, with nitrate anions coordinating in a monodentate manner at O-Cd bond lengths of 2.315(7) and 2.343(9) Å. In addition, and similarly to complexes **1m** and **1p**, above, host-guest interactions are present between the electron rich CTV core and a DMF molecule, whereby the non-polar *N*-methyl moiety is directed towards the centre of the cavitand host.

Akin to complex **1p**, the complex also features aggregation of hydrophobic **L1p** propyl chains. The *cis*-coordinated **L1p** ligands are orientated in a head-to-head manner, affording an off-set, cylindrical arrangement, where opposing ligands are opposite enantiomers and thus the network is a racemate. Any resultant free space is filled with diethyl-ether and DMF solvent. This cylindrical motif gives rise to 4-gons within the resultant 2D net, which are extended 2-dimensionally through coordination of the third independent **L1p** ligand about the *fac*-Cd(II) centre. Thus, the network comprises a series of linked 4- and 8-gons to afford a $4\cdot 8^2$ topology, where both ligand and metal centres represent 3-connected

nodes. The formation of these 2D sheets is facilitated through intermolecular interactions, whereby the methylene protons of the cyclononatriene core hydrogen bond to the electron rich upper rim of the CTG core, displaying C-H···O separations of 3.105 and 3.185 Å. In addition, the core aromatics of the [*a,d,g*]cyclononatriene scaffold highlight π-π interactions with neighbouring pyridyl functions and display off-set centroid separations of 3.741 Å. Individual 2D sheets close-pack, in the absence of intermolecular interactions, to construct the extended network. The proposed network composition was fully concordant with elemental analysis and IR spectroscopy.

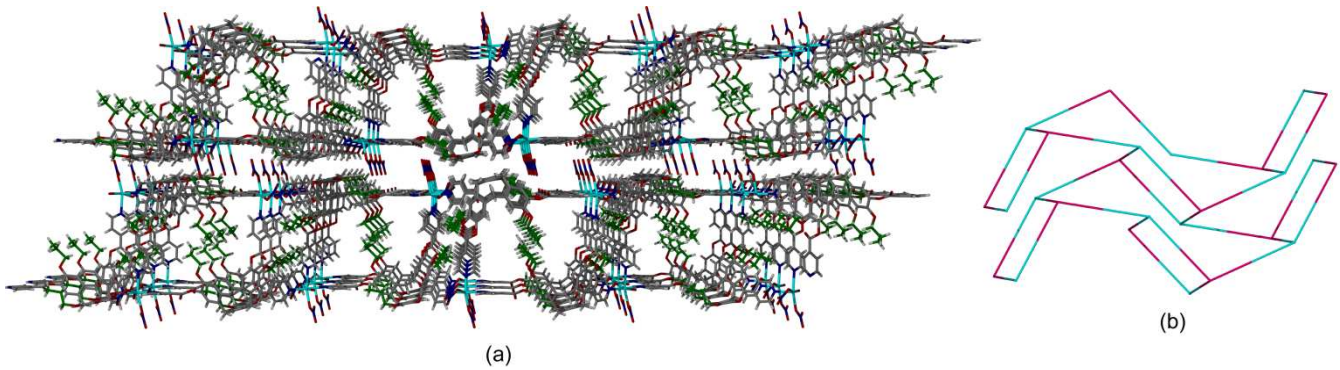

Fig. 2 From the crystal structure of complex **2p**. (a) As viewed down the crystallographic *b* axis, depicting the inwardly orientated head-to-head orientation of individual **L1p** ligands giving rise to aggregation of the hydrophobic propyl chains across each 2D sheet. Propyl chains displayed in green and all solvent molecules are omitted for clarity; (b) the simplified connectivity diagram, where the blue and pink spheres are metal and ligand, respectively. The resultant 4- and 8-gons giving rise to the overall $4{\cdot}8^2$ network topology. Only one ligand disorder position is shown for clarity.

An analogous complex to **2p** but with ligand **L1m** in place of **L1p** was not formed. In fact, we did not isolate any cadmium(II) complexes of **L2m**. This may be solubility driven, whereby the added solubility of **L1p** ligands facilitate the self-assembly in solution and prevents random oligomerisation of the starting components. A further factor may be the large van der Waals interactive surface that is present between individual **L1p** ligands. Such interactions, observed for both complex **1p** and **2p**, are in keeping with the results of Cockroft and co-workers, confirming the driving force for alkyl-alkyl interactions based on the solvophobic effect.[34]

2.2 The role of solubility and sterics

We have previously reported that *tris*-(2-quinolylmethyl)cyclotriguaiacylene **L2m** forms an unusual twisted tetrahedral structure with silver(I) cations, $[Ag_4(\mathbf{L2m})_4]{\cdot}4(BF_4)$, complex **3m**, Figure 3.[47] Complex **3m** is close-packed and displays a hydrophobic core with four inwardly pointing methyl moieties in close proximity to one another. Despite our best efforts, metallo-supramolecular constructs were not identified to form from **L2m** with other transition metals. Whilst methylated ligand **L2m** forms a discrete, tetrameric cube with Ag(I) cations, reactions of the propylated congener **L2p** under the same conditions did not. This is as expected, however, due to the larger propyl groups not being able to be accommodated within the close-packed core of the Ag_4L_4 tetrahedron. A complex was formed from the propylated ligand and Ag(I), however, with the stoichiometric reaction of **L2p** and $Ag[Co(C_2B_9H_{11})_2]$ resulting in the formation of a 1D coordination polymer, $\{[Ag\,Ag(\mathbf{L2p})[Co(C_2B_9H_{11})_2]]{\cdot}1.5(MeNO_2)\}_\infty$, complex **3p**. Crystals were obtained from a nitromethane ($MeNO_2$) solution and were small, twinned and weakly diffracting; nevertheless, a data collection was made using synchrotron radiation and the structure solved in the monoclinic space group $P2_1/c$.

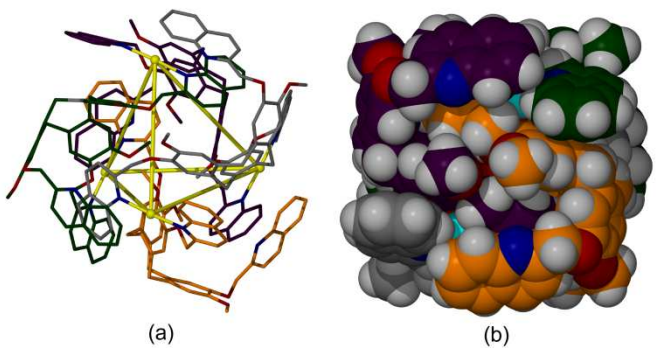

Fig. 3 Crystal structure of the previously reported complex $[Ag_4(\mathbf{L2m})_4]^{4+}$, **3m**. (a) Highlighting the twisted tetrahedral core, and (b) space-filling diagram displaying the resultant cube-like appearance.[47]

The asymmetric unit contains two molecules of ligand **L2p**, two Ag(I) cations, and two $[Co(C_2B_9H_{11})_2]^-$ counter anions, alongside nitromethane solvent. The 1D coordination polymer formed is a racemate and features the inclusion of both enantiomers of **L2p** ligands *per* 1D chain, Figure 4. Ligands have approximate C_3-symmetry and coordinate two Ag(I) cations, with one ligand arm remaining uncoordinated, akin to complex **3m**. Each Ag(I) cation is approximately linear and is coordinated by two independent **L2p** ligands, with N-Ag bond lengths and N-Ag-N angles of 2.189(7)-2.197(7) Å and 174.3(3) and 176.2(3) °, respectively. There is some bonding contribution from a proximal ethereal oxygen, with O···Ag separation of 2.513(7) Å. In a similar manner to complex **3m**, this system also displays host-guest interactions between quinolyl arm and the shallow hydrophobic cavity of the ligand core; however, in this instance the interaction is not reciprocal

 This journal is © The Royal Society of Chemistry 2012

and instead is unidirectional along the length of each 1D chain, Figure 4b.

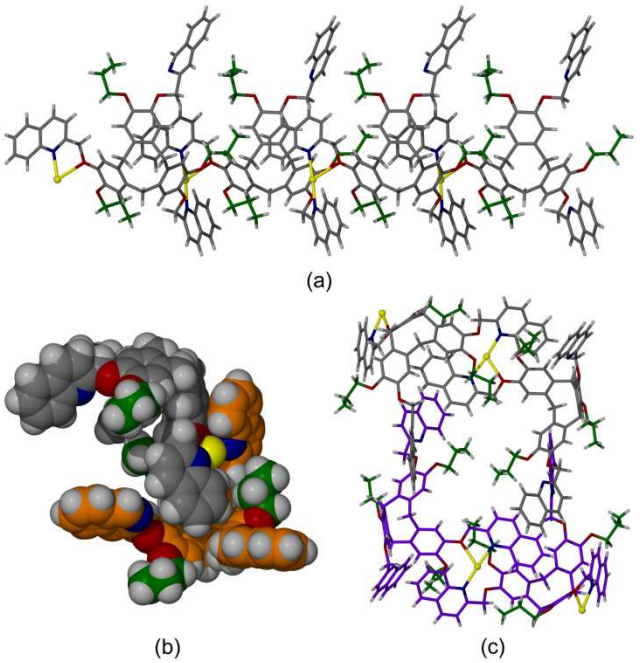

Fig. 4 From the crystal structure of complex **3p**. (a) Displaying an individual {[Ag(**L1p**)]}$_\infty$ 1D polymer unit; (b) Intra-polymer Quinolyl-CTG aromatic interactions that are present along the length of individual 1D chains. Independent ligands are colour-coded for clarity; (c) Interstrand aggregation of propyl chains across neighbouring 1D polymers. Individual 1D chains are colour coded, propyl moieties are shown in green and anions and solvent are omitted for clarity.

This interaction is further stabilised by π···π interactions between the quinolyl moiety and [*a,d,g*]cyclononatriene core, with centroid separation of 3.809 Å, Figure 4. Neighbouring 1D chains aggregate through π···π interactions, with aromatic centroid separations of 3.687 Å, and aggregation of propyl moieties which affords small pockets that are filled with disordered solvent and $[Co(C_2B_9H_{11})_2]^-$ anions, Figure 4c. Whilst there are similarities to be noted, such as host-guest interactions and complex stoichiometry, it is ultimately the presence of sterically demanding propyl chains that renders the formation of the M_4L_4 tetramer seen with ligand **L2m** improbable.

Comparatively, methylated ligand **L2m** was not seen to form coordination complexes with palladium(II) salts, whereas its more soluble propylated congener resulted in the formation of an unusual, compressed $[Pd_6(\mathbf{L2p})_4]^{12+}$ assembly.

The reaction of two equivalents of propylated **L2p** with three equivalents of $Pd(CF_3CO_2)_2$ in an acetonitrile, nitromethane and water solvent mixture gave a discrete, hexanuclear assembly complex $[Pd_6(\mathbf{L2p})_4(CF_3CO_2)_{12}]\cdot(Et_2O)$ **4p** on diffusion of diethyl-ether anti-solvent. Once formed, the complex was highly insoluble in most common solvents and was isolated as an inhomogeneous, amorphous/crystalline yellow solid. Suitable single crystals were isolated from the bulk product and were small and weakly diffracting; nevertheless, a solution was obtained in the monoclinic space group *C*2/*c*. The asymmetric unit comprises half the overall complex and features two crystallographically distinct **L2p** ligands, three inequivalent palladium(II) centres and six coordinating trifluoroacetate anions, alongside half a molecule of diethyl-ether. The two ligands in the asymmetric unit are of the opposite enantiomer to one another which results in a *meso*-complex, akin to complex **3m**.[47]

Pd(II) centres are square planar and are exclusively *trans* coordinated by the quinolyl donors and display Pd-N bond lengths in the range 2.051(6)-2.070(7) Å and N-Pd-N angles of 176.3(3), 177.2(3) and 177.5(4)°. Two trifluoroacetate anions coordinate each palladium(II) centre to render the overall complex charge-neutral and display Pd-O bond lengths ranging 1.971(7)-2.060(9) Å, and O-Pd-O angles of 172.5(3), 175.0(3) and 176.5(3) °, Figure 5. Interestingly, the use of trifluoroacetate anion was integral to complex formation and the complex did not form with other coordinating anions, such as nitrate or acetate.

Complex **4p** is centrosymmetric and displays both host-guest and π-π interactions, but has no internal space, Figure 5. Two sets of off-set, clathrate-type, bowl-in-bowl **L2p** stacking pairs are observed within the complex, where the methylene protons of the [*a,d,g*]cyclononatriene core are directed towards the hydrophobic bowl of the underside of a ligand forming C-H···π interactions at 2.54 Å, akin to the stacking arrangement found in *β*-phase clathrates of CTV.[53] The host-guest interactions displayed in complex **4p** are opposite to those found in complex **3m**, which highlighted a propensity for the quinolyl arm to interact with the [*a,d,g*]cyclononatriene core. However, whilst the modes of intramolecular interaction may differ, the result in each case is a tetrameric *meso*-complex that exists as a racemic dimer of dimers.[47]

Each **L2p** ligand binds to three Pd(II) centres, and the two symmetry related quinolyl groups in the centre of the $[Pd_6(\mathbf{L2p})_4\cdot(CF_3CO_2)_{12}]$ assembly form phenyl···pyridyl, face-to-face, π-π stacking interactions at a ring centroid separation of 3.75 Å. This is again converse to the coordination stoichiometry found in complex **3m**, where only two ligand arms coordinated the metal centres.[47]

Van der Waals dispersion interactions are again present between neighbouring propyl chains, yet to a much lesser extent than for complexes constructed from ligand **L1p**. This is perhaps due to the numerous aromatic interactions afforded through the quinolyl moieties.

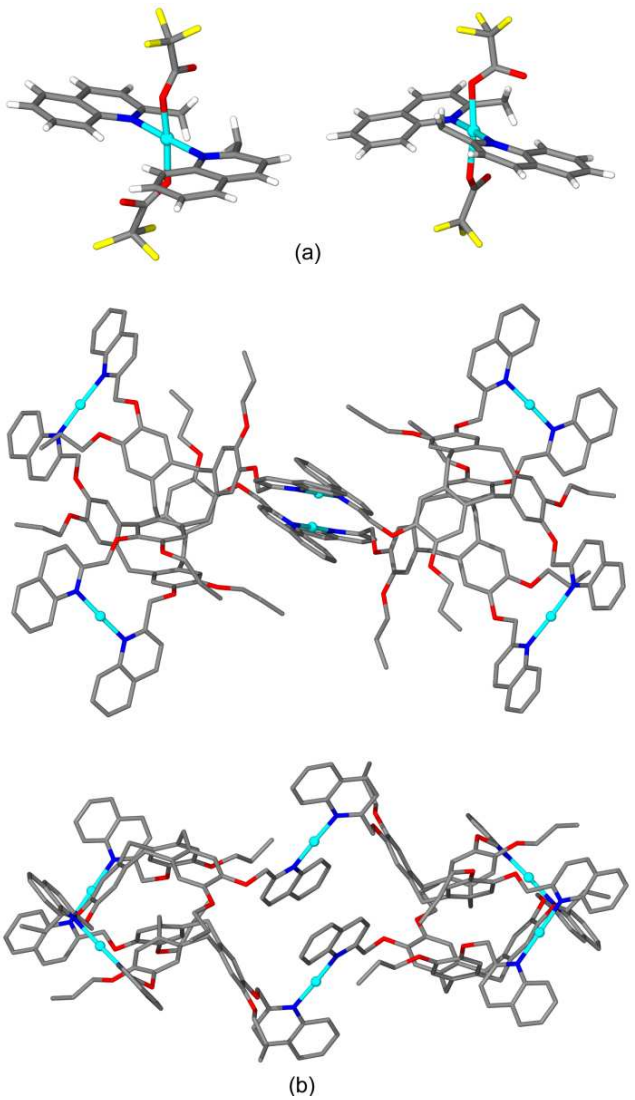

Fig. 5 From the crystal structure of complex **4p** (a) The two types of Pd(II) coordination environments showing *trans*, *cis* and *trans*, *trans* quinolyl arrangements; (b) two views of the of $[Pd_6(\mathbf{L2p})_4]^{12+}$ assembly, anions are omitted and disordered propyl chains shown in only one position for the sake of clarity.

There are two Pd(II) coordination modes within the complex. For two symmetry related Pd(II) cations, the *trans* quinolyl ligands are not mutually co-planar and are arranged such that their phenyl rings are *trans* to one another. The other four Pd(II) ions each have a co-planar arrangement of the two coordinating quinolyl moieties, which display mirror-like symmetry and hence a *cis* arrangement of the phenyl groups. Previously reported examples of M_6L_4 metallo-supramolecular assemblies are Fujita's $[Pd_6(en)_6L_4]^{12+}$ cages, where en = ethylenediamine,[54] or variants.[55,56] In these, the metal centres are arranged in an octahedron with flat tripodal ligands, such as *tris*(4-pyridyl)triazine, bridging between them. The ligands are arranged *cis* to one another and occupy half of the octahedral faces through vertex sharing, shown in cartoon form in Figure 6a.

Complex **4p** can also be understood in terms of an octahedron with half the faces taken up by the tripodal ligand, however the octahedron is significantly compressed, and the ligands are both vertex and edge-sharing, Figure 6b. This is not the first CTV-derived complex that is built on an octahedral framework and we have previously reported the elucidation and solution-phase behavior of a family of $[Pd_6L_8]^{12+}$ octomeric assemblies with 4-pyridyl-derived ligands.[39,57]

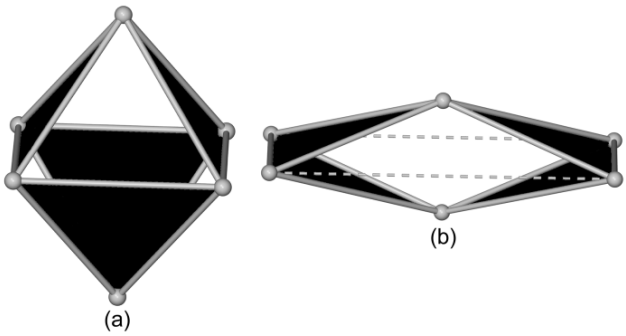

Fig. 6 Comparison of Pd_6L_4 assemblies, spheres represent Pd(II) positions taken from crystal structures, while shaded faces show positioning of tripodal ligands. (a) Fujita's octahedral $[Pd_6(en)_6L_4]^{12+}$ assembly with vertex sharing L = *tris*(4-pyridyl)triazine;[54] (b) $[Pd_6(\mathbf{L2p})_4(CF_3CO_2)_{12}]$ assembly with vertex and edge-sharing of ligand positions.

The extended lattice of complex **4p** possesses two sites of void space which contain disordered lattice solvent, comprising a head-to-head arrangement of ligands between neighbouring complexes and large, unidirectional channels that run down the crystallographic *c*-axis (Figure 7). The insolubility of complex **4p** meant that its solution-phase behaviour could not be probed. ESI-MS analyses were conducted in DMSO but no peaks corresponding to the complex were observed and it is likely that it undergoes a coordination-induced disassembly.

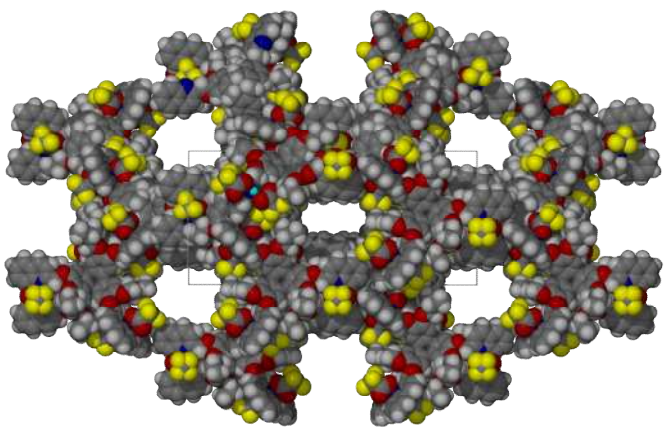

Fig. 7 The extended structure of complex **4p**, as viewed down the crystallographic *c* axis, depicting the large, unidirectional channels.

It is interesting to note that all attempts to form the analogous Pd_6L_4 assembly with methylated ligand **L2m** were unsuccessful. Equally, the analogous $Ag_6(\mathbf{L2p})_4$ complex was inaccessible, in spite of the linear coordination geometry required. It appears that complexes **3m**, **3p** and **4p** are all

 This journal is © The Royal Society of Chemistry 2012

unique and highly specific with respect to their preference for metal salt used.

3. Experimental

General

Chemicals were obtained from commercial sources and used without further purification. Propylated-cyclotriguaiacylene (*p*-CTG) was prepared according to literature methods from propyl-cyclotriveratrylene (*p*-CTV).[46,58] Ligands **L1m**, **L1p** and **L2m** were prepared according to known literature procedures.[46,47,49] NMR spectra were recorded by automated procedures on a Bruker DPX 500 or 300 MHz NMR spectrometer. Electrospray mass spectra (ESI-MS) were measured on a Bruker MicroTOF-Q or Bruker MaXis Impact instruments in positive ion mode. Infra-red spectra were recorded as solid phase samples on a Perkin-Elmer FT-IR Spectrometer and microanalyses were performed by the University of Leeds microanalytical service using a Carlo Erba Elemental Analyser MOD 1106 spectrometer. Samples for microanalysis were dried under vacuum prior to analysis.

Preparation of compounds

(±)-2,7,12-Tripropoxy-3,8,13-*tris*(2-quinolylmethyl)-10,15-dihydro-5*H*-tribenzo[*a,d,g*]cyclononene (L2p) A mixture of *p*-CTG (369 mg, 0.749 mmol) and potassium carbonate (1.24 g, 8.99 mmol) were held at reflux in acetonitrile (150 mL), under argon, for thirty minutes. After which, 2-(chloromethyl)quinoline hydrochloride (0.99 g, 4.49 mmol) was added and the reaction mixture held at reflux for a further 48 hours. The reaction mixture was cooled to room temperature and solvent removed *in vacuo*. The resultant residue was taken up into dichloromethane (150 mL), washed with water (2 × 50 mL) and brine (50 mL), dried over $MgSO_4$ and concentrated *in vacuo*. The desired compound was obtained as a white solid through trituration of the impure material with methanol, collected by filtration and dried *in vacuo*. Yield 863 mg, 89 %. m.p. decomposes > 230 °C; HRMS (ES^+): *m/z* 916.4334 $\{MH\}^+$; calculated for $C_{60}H_{58}N_3O_6$ 916.4326; ^1H NMR (300MHz, $CDCl_3$) δ (ppm) = 8.17 (d, 3H, quin-H^4, *J* = 8.5 Hz), 8.07 (d, 3H, quin-H^3, *J* = 8.5 Hz), 7.83 (d, 3H, quin-H^6, *J* = 7.2 Hz), 7.77-7.71 (m, 6H, quin-H^8, H^9), 7.55 (dd, 3H, quin-H^7, *J* = 7.0, 8.1 Hz), 6.93 (s, 3H, aryl-H), 6.74 (s, 3H, aryl-H), 5.39 (s, 6H, OC$\underline{H}_2$-quin), 4.67 (d, 3H, CTG *exo*-H, *J* = 13.8 Hz), 3.80 (m, 6H, propyl -H, *J* = 6.4 Hz), 3.43 (d, 3H, CTG *endo*-H, *J* = 13.8 Hz), 1.72 (q, 6H, propyl β-H, *J* = 6.8 Hz), 0.97 (t, 9H, propyl -H, *J* = 7.4 Hz); $^{13}C\{^1H\}$ NMR (75 MHz, $CDCl_3$) δ (ppm) = 158.7, 147.9, 147.5, 147.1, 136.9, 132.9, 131.7, 129.7, 128.8, 127.8, 127.6, 126.4, 119.1, 116.3, 115.3, 72.7, 70.6, 36.5, 22.6, 10.6; Analysis for **L2p**·2.5(H_2O) (% calculated, found) C (74.99, 75.20), H (6.49, 6.10), N (4.37, 4.35); Infrared analysis (FT-IR, cm^{-1}) 3400-3100 (broad), 2925, 1600, 1506, 1265, 1140, 1093.

$\{[Ag(L1p)[Co(C_2B_9H_{11})_2]]\cdot 2.5(DMF)\cdot(H_2O)\}_\infty$ (complex 1p) $Ag[Co(C_2B_9H_{11})_2]$ (6.43 mg, 0.0149 mmol) and **L1p** (12.10 mg, 0.0149 mmol) were dissolved in DMF (~ 1 mL) and diethyl-ether vapours were diffused into the solution. Yellow blocks formed after 21 days and were analyzed *via* single crystal X-ray analysis using a synchrotron source. Yield 7.4 mg. Analysis for $\{[Ag(\mathbf{L1p})[Co(C_2B_9H_{11})_2]]\cdot 2(DMF)\cdot 2(H_2O)\}_\infty$ (% calculated, found) C (49.00, 49.20), H (6.03, 6.20), N (4.93, 5.05). Infrared analysis (FT-IR, cm^{-1}) 2985, 2810, 1750, 1664, 1504, 1271, 1106, 756.

$\{[Cd(L1p)(NO_3)_2(H_2O)]\cdot(DMF)\cdot 0.5(Et_2O)\}_\infty$ (complex 2p) $Cd(NO_3)_2\cdot 4H_2O$ (6.89 mg, 0.0224 mmol) and **L1p** (12.10 mg, 0.0149 mmol) were dissolved in DMF (~ 1 mL) and diethyl-ether vapours were diffused into the solution. Colourless needles formed after 21 days and were analyzed *via* single crystal X-ray analysis. Yield 4.9 mg. Analysis for $\{[Cd(\mathbf{L1p})\cdot(NO_3)_2\cdot(DMF)]\cdot(DMF)\cdot 4(H_2O)\}_\infty$ (% calculated, found) C (51.37, 51.55), H (5.35, 5.00), N (7.77, 7.80). Infrared analysis (FT-IR, cm^{-1}) 3400-3150 (broad), 2965, 2914, 1777, 1654, 1509, 1480-1400 (broad), 1261, 758.

$\{[Ag_2(L2p)_2][Co(C_2B_9H_{11})_2]_2\cdot 1.5(MeNO_2)\}_\infty$ (complex 3p) Ag(cobalt(III)*bis*(dicarbollide)) (6.43 mg, 0.0149 mmol) and **L2p** (13.60 mg, 0.0149 mmol) were dissolved in a 1:1 mixture of acetonitrile and nitromethane (~ 1.2 mL) and diethyl-ether vapours were diffused into the solution. Small, orange blocks formed after 28 days and were analyzed *via* single crystal X-ray analysis using a synchrotron source. Yield 6.6 mg. Analysis for $\{[Ag_2(\mathbf{L2p})_2][Co(C_2B_9H_{11})_2]_2\}_\infty$ (% calculated, found) C (57.04, 56.90), H (5.91, 6.00), N (3.12, 3.00); Infrared (FT-IR, cm^{-1}) 2963, 2551, 1599, 1510, 1255, 1143, 1086, 980, 824, 760.

$[Pd_6(L2p)_4(CF_3CO_2)_{12}]\cdot n(CH_3NO_2)\cdot n(Et_2O)$ (complex 4p) $Pd(CF_3CO_2^-)_2$ (6.89 mg, 0.0224 mmol) and **L2p** (12.10 mg, 0.0149 mmol) were dissolved in a 1:1 mixture of acetonitrile and nitromethane (~ 1 mL) and diethyl-ether vapour was diffused into the solution to give bulk crystalline material. Yield 1.8 mg. Analysis for $[Pd_6(\mathbf{L2p})_4(CF_3CO_2^-)_{12}]\cdot 3(CH_3NO_2)\cdot 7(H_2O)$ (% calculated, found) C (53.73, 53.40), H (4.24, 4.15), N (3.52, 3.20); Infrared analysis (FT-IR, cm^{-1}) 2991, 1747, 1605, 1501, 1269, 1178 (CF_3CO_2 anion), 1146 (CF_3CO_2 anion). ^1H NMR resonances of the complex were broad and unassignable and the mass spectra did not highlight any mass peaks corresponding to the molecular ion or its breakdown. Larger crystals grown for single crystal X-ray analysis were isolated using a similar procedure but with a 2:2:1 mixture of acetonitrile:nitromethane:water as the solvent system.

Crystallography

Crystals were mounted on a glass or MiTeGen fibre tip under oil and flash frozen using a stream of cold N_2. Data were collected on a Bruker-Nonius X8 diffractometer with an Mo-rotating anode (λ = 0.71073 Å), or on a Rigaku Saturn using synchrotron radiation (λ = 0.6899 Å) at station I19 at Diamond Light Source. Data were

corrected for Lorenztian and polarization effects and absorption corrections were applied using multi-scan methods. The structures were solved by direct methods using SHELXS-97 and refined by full-matrix least-squares on F^2 using SHELXL-97, aside from complex **3p** which was refined by block-matrix least-squares, interfaced through the X-seed interface.[59,60] Unless otherwise specified, all non-hydrogen atoms were refined as anisotropic, and hydrogen positions were included at geometrically estimated positions. Molecular graphics were obtained using POV-RAY through the X-Seed interface.[60] Additional details of data collections and refinements are summarised below and details of disorder treatment are given in Supplementary Information.

$\{[Ag(L1p)[Co(C_2B_9H_{11})_2]]\cdot 2.5(DMF)\cdot(H_2O)\}_\infty$ 1p: $C_{118}H_{173}Ag_2B_{36}Co_2N_{11}O_{25}$, Mr = 2880.44, triclinic, a = 10.324(3), b = 18.828(5), c = 21.852(6) Å, α = 69.016(6), β = 84.428(10), γ = 75.039(10) °, V = 3831.3(18) Å^3, synchrotron radiation, space group P-1, Z = 1, θ_{max} = 26.57 °, T = 100(1) K, 869 parameters, 4 restraints, R_1 = 0.0807 (for 13623 data $I > 2\sigma(I)$), wR_2 = 0.2426 (all 15549 data). CCDC-988765.

$\{[Cd(L1p)(NO_3)_2(H_2O)]\cdot(DMF)\cdot 0.5(Et_2O)\}_\infty$ 2p: $C_{106}H_{118}Cd_2N_{12}O_{35}$, Mr = 2344.92, monoclinic, a = 38.700(3), b = 9.6729(10), c = 38.853(4) Å, β = 111.954(4) °, V = 13490(2) Å^3, space group $C2/c$, Z = 4, θ_{max} = 24.69 °, T = 150(1) K, 736 parameters, 755 restraints, R_1 = 0.1335 (for 7036 data $I > 2\sigma(I)$), wR_2 = 0.4291 (all 11416 data). CCDC-988766.

$[Ag_2(L2p)_2][Co(C_2B_9H_{11})_2]_2\cdot 1.5(MeNO_2)\}_\infty$ 3p: $C_{129.5}H_{163.5}Ag_2B_{36}Co_2N_{7.5}O_{15}$, Mr = 2787.94, monoclinic, a = 19.3628(7), b = 43.7924(11), c = 16.6371(6) Å, β = 90.525(3) °, V = 14107.7(8) Å^3, synchrotron radiation, space group $P2_1/c$, Z = 4, θ_{max} = 22.50 °, T = 100(1) K, 1633 parameters, 2 restraints, R_1 = 0.1128 (for 15562 data $I > 2\sigma(I)$), wR_2 = 0.3462 (all 20256 data). CCDC-988767

$[Pd_6(L2p)_4(CF_3CO_2)_{12}]\cdot(Et_2O)$ 4p: $C_{268}H_{234}F_{36}N_{12}O_{49}Pd_6$, Mr = 5729.07, monoclinic, a = 21.057(5), b = 44.917(9), c = 40.687(8) Å, β = 97.365(6) °, V = 38165(14) Å^3, space group $C2/c$, Z = 4, θ_{max} = 20.00 °, T = 150(1) K, 1368 parameters, 26 restraints, R_1 = 0.0914 (for 10804 data $I > 2\sigma(I)$), wR_2 = 0.2572 (all 17764 data). The SQUEEZE[61] routine of PLATON[62] was employed on this structure. CCDC-955888.

4. Conclusions

In summary, we have shown how two cyclotriveratrylene ligand pairs, differing only in the length of alkoxy substituents, display dissimilar metal-mediated self-assembly even under analogous conditions. Such sterically and interactionally similar ligand pairs demonstrate how even subtle alterations to the organic building blocks are enough to bias their self-assembly.

The self-assembly of a methylated and propylated 4-pyridyl-derived ligand pair, **L1m** and **L1p**, was dependent on aggregation of propyl moieties as a driving force in complex formation, resulting in expansion of a 2-connected 1D polymer, as for methylated ligand **L1m**, to a 3-connected 1D polymer for propylated ligand **L1p**. This was mirrored in the formation of a 2D net with cadmium(II) centres, featuring two sites of alkyl-alkyl interactions, that was inaccessible with the methylated ligand.

Similar results were found for the 2-quinolyl ligand pair, **L2m** and **L2p**, whereby the formation of the $[Ag_4(\mathbf{L1m})_4]^{4+}$ tetramer was prevented due to sterics; and how the increased solubility of propylated ligand **L1p** allows for the elucidation of a new type of compressed, hexameric $[Pd_6(\mathbf{L1p})_4]^{12+}$ assembly that is inaccessible with parent, methylated ligand **L1m**.

5. Acknowledgements

The authors thank the EPSRC, Charles Brotherton Trust and the University of Leeds for funding and Ian Blakely for microanalytical measurements. This work was carried out in collaboration with Diamond Light Source, using beamline I19, under proposal numbers mt7847 and mt8517.

6. Notes and references

School of Chemistry, University of Leeds, Woodhouse Lane, Leeds, LS2 9JT, UK. Email: m.j.hardie@leeds.ac.uk.

† Electronic Supplementary Information (ESI) available: Details of synthetic methodology and further crystallographic details. For ESI and crystallographic data in CIF or other electronic format see DOI: 10.1039/b000000x/

1. J. M. Lehn, *Angew. Chem., Int. Ed. Engl.*, 1988, **27**, 89-112.
2. G. M. Whitesides and B. Grzybowski, *Science*, 2002, **295**, 2418-2421.
3. H.-C. Zhou, J. R. Long and O. M. Yaghi, *Chem. Rev.*, 2012, **112**, 673-674.
4. T. R. Cook, Y.-R. Zheng and P. J. Stang, *Chem. Rev.*, 2012, **113**, 734-777.
5. R. Chakrabarty, P. S. Mukherjee and P. J. Stang, *Chem. Rev.*, 2011, **111**, 6810-6918.
6. C. J. Hastings, M. D. Pluth, R. G. Bergman and K. N. Raymond, *J. Am. Chem. Soc.*, 2010, **132**, 6938-6940.
7. D. Fiedler, H. van Halbeek, R. G. Bergman and K. N. Raymond, *J. Am. Chem. Soc.*, 2006, **128**, 10240-10252.
8. Y. Kohyama, T. Murase and M. Fujita, *J. Am. Chem. Soc.*, 2014, **136**, 2966-2969.
9. Y. Inokuma, M. Kawano and M. Fujita, *Nat. Chem.*, 2011, **3**, 349-358.
10. Y. Jiao, J. Wang, P. Wu, L. Zhao, C. He, J. Zhang and C. Duan, *Chem.-Eur. J.*, 2014, **20**, 2224-2231.
11. Y. Inokuma, S. Yoshioka, J. Ariyoshi, T. Arai, Y. Hitora, K. Takada, S. Matsunaga, K. Rissanen and M. Fujita, *Nature*, 2013, **495**, 461-466.
12. P. Mal, B. Breiner, K. Rissanen and J. R. Nitschke, *Science*, 2009, **324**, 1697-1699.
13. M. J. Wiester, P. A. Ulmann and C. A. Mirkin, *Angew. Chem., Int. Ed.*, 2011, **50**, 114-137.
14. M. M. J. Smulders, I. A. Riddell, C. Browne and J. R. Nitschke, *Chem. Soc. Rev.*, 2013, **42**, 1728-1754.
15. S. De, K. Mahata and M. Schmittel, *Chem. Soc. Rev.*, 2010, **39**, 1555-1575.

 This journal is © The Royal Society of Chemistry 2012

16. S. P. Argent, H. Adams, T. Riis-Johannessen, J. C. Jeffery, L. P. Harding and M. D. Ward, *J. Am. Chem. Soc.*, 2006, **128**, 72-73.
17. M. D. Levin and P. J. Stang, *J. Am. Chem. Soc.*, 2000, **122**, 7428-7429.
18. S. Freye, D. M. Engelhard, M. John and G. H. Clever, *Chem.-Eur. J.*, 2013, **19**, 2114-2121.
19. S. Freye, R. Michel, D. Stalke, M. Pawliczek, H. Frauendorf and G. H. Clever, *J. Am. Chem. Soc.*, 2013, **135**, 8476-8479.
20. Q.-F. Sun, J. Iwasa, D. Ogawa, Y. Ishido, S. Sato, T. Ozeki, Y. Sei, K. Yamaguchi and M. Fujita, *Science*, 2010, **328**, 1144-1147.
21. Y.-R. Zheng and P. J. Stang, *J. Am. Chem. Soc.*, 2009, **131**, 3487-3489.
22. Y.-R. Zheng, W.-J. Lan, M. Wang, T. R. Cook and P. J. Stang, *J. Am. Chem. Soc.*, 2011, **133**, 17045-17055.
23. S. J. Park, D. M. Shin, S. Sakamoto, K. Yamaguchi, Y. K. Chung, M. S. Lah and J.-I. Hong, *Chem.-Eur. J.*, 2005, **11**, 235-241.
24. R. L. Paul, Z. R. Bell, J. C. Jeffery, J. A. McCleverty and M. D. Ward, *Proc. Natl. Acad. Sci. U. S. A.*, 2002, **99**, 4883-4888.
25. F. London, *Transactions of the Faraday Society*, 1937, **33**, 8b-26.
26. F. London, *Z. Physik*, 1930, **63**, 245-279.
27. C. Piguet, *Dalton Trans.*, 2011, **40**, 8059-8071.
28. C. Piguet, *Chem. Commun.*, 2010, **46**, 6209-6231.
29. J. Hamacek, M. Borkovec and C. Piguet, *Dalton Trans.*, 2006, 1473-1490.
30. D. Chandler, *Nature*, 2005, **437**, 640-647.
31. T. P. Silverstein, *J. Chem. Ed.*, 1998, **75**, 116.
32. N. H. Joh, A. Oberai, D. Yang, J. P. Whitelegge and J. U. Bowie, *J. Am. Chem. Soc.*, 2009, **131**, 10846-10847.
33. J. A. Thomas, *Nat. Chem.*, 2009, **1**, 25-26.
34. L. Yang, C. Adam, G. S. Nichol and S. L. Cockroft, *Nat. Chem.*, 2013, **5**, 1006-1010.
35. S. T. Mough and K. T. Holman, *Chem. Commun.*, 2008, 1407-1409.
36. J. J. Henkelis, S. A. Barnett, L. P. Harding and M. J. Hardie, *Inorg. Chem.*, 2012, **51**, 10657-10674.
37. J.-T. Yu, J. Sun. Z.-T. Huang, Q.-Y. Zheng, *CrystEngComm*, 2012, **14**, 112-115.
38. C. J. Sumby and M. J. Hardie, *Angew. Chem., Int. Ed.*, 2005, **44**, 6395-6399.
39. T. K. Ronson, J. Fisher, L. P. Harding and M. J. Hardie, *Angew. Chem., Int. Ed.*, 2007, **46**, 9086-9088.
40. Z. Zhong, A. Ikeda, S. Shinkai, S. Sakamoto and K. Yamaguchi, *Org. Lett.*, 2001, **3**, 1085-1087.
41. B. F. Abrahams, B. A. Boughton, N. J. FitzGerald, J. L. Holmes and R. Robson, *Chem. Commun.*, 2011, **47**, 7404-7406.
42. B. F. Abrahams, N. J. FitzGerald and R. Robson, *Angew. Chem., Int. Ed.*, 2010, **49**, 2896-2899.
43. A. Westcott, J. Fisher, L. P. Harding, P. Rizkallah and M. J. Hardie, *J. Am. Chem. Soc.*, 2008, **130**, 2950-2951.
44. J. J. Henkelis, T. K. Ronson, L. P. Harding and M. J. Hardie, *Chem. Commun.*, 2011, **47**, 6560-6562.
45. T. K. Ronson, J. Fisher, L. P. Harding, P. J. Rizkallah, J. E. Warren and M. J. Hardie, *Nat. Chem.*, 2009, **1**, 212-216.
46. J. J. Henkelis, S. L. Warriner, J. Fisher and M. J. Hardie, *Chem.-Eur. J.*, 2014, **20**, 4417-4125.
47. C. Carruthers, T. K. Ronson, C. J. Sumby, A. Westcott, L. P. Harding, T. J. Prior, P. Rizkallah and M. J. Hardie, *Chem.-Eur. J.*, 2008, **14**, 10286-10296.
48. M. J. Hardie and C. J. Sumby, *Inorg. Chem.*, 2004, **43**, 6872-6874.
49. M. J. Hardie, R. M. Mills and C. J. Sumby, *J. Org. Biol. Chem.*, 2004, **2**, 2958-2964.
50. T. Moriuchi-Kawakami, J. Sato and Y. Shibutani, *Anal. Sci.*, 2009, **25**, 449-452.
51. L. Cunha-Silva, R. Ahmad and M. J. Hardie, *Aust. J. Chem.*, 2006, **59**, 40-48.
52. D.-L. Long, A. J. Blake, N. R. Champness, C. Wilson and M. Schröder, *Angew. Chem., Int. Ed.*, 2001, **40**, 2444-2447.
53. J. W. Steed, H. Zhang and J. L. Atwood, *Supramol. Chem.*, 1996, **7**, 37-45.
54. M. Fujita, D. Oguro, M. Miyazawa, H. Oka, K. Yamaguchi and K. Ogura, *Nature*, 1995, **378**, 469-471.
55. S. Leininger, J. Fan, M. Schmitz and P. J. Stang, *Natl. Acad. Sci. U. S. A.*, 2000, **97**, 1380-1384.
56. O. Chepelin, J. Ujma, X. Wu, A. M. Z. Slawin, M. B. Pitak, S. J. Coles, J. Michel, A. C. Jones, P. E. Barran and P. J. Lusby, *J. Am. Chem. Soc.*, 2012, **134**, 19334-19337.
57. T. K. Ronson, C. Carruthers, J. Fisher, T. Brotin, L. P. Harding, P. J. Rizkallah and M. J. Hardie, *Inorg. Chem.*, 2010, **49**, 675-685.
58. R. Ahmad and M. J. Hardie, *Supramol. Chem.*, 2006, **18**, 29-38.
59. G. Sheldrick, *Acta Crystallogr., Sect. A*, 2008, **64**, 112-122.
60. L. J. Barbour, *Supramol. Chem.*, 2001, **1**, 189-191.
61. A. L. Spek, *Acta. Crystallogr., Sect. A*, 1990, **A46**.
62. A. L. Spek, *Acta. Crystallogr., Sect. D*, 2009, **46**, 194.

Graphical Abstract

Propylated cyclotriveratrylene ligands with N-donor groups form coordination polymers where the propyl groups aggregate or form a Pd_6L_4 cage.

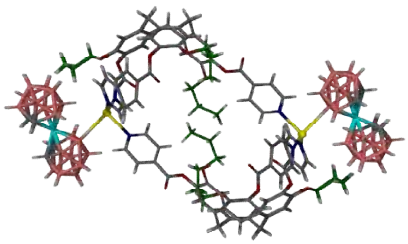

This journal is © The Royal Society of Chemistry 2012